Global ab initio ground-state potential energy surface of N4

Yuliya Paukku, Ke R. Yang, Zoltan Varga, and Donald G. Truhlar

Citation: J. Chem. Phys. **139**, 044309 (2013); doi: 10.1063/1.4811653
View online: http://dx.doi.org/10.1063/1.4811653
View Table of Contents: http://jcp.aip.org/resource/1/JCPSA6/v139/i4
Published by the AIP Publishing LLC.

Global *ab initio* ground-state potential energy surface of N_4

Yuliya Paukku, Ke R. Yang, Zoltan Varga, and Donald G. Truhlar[a)]
Department of Chemistry, Chemical Theory Center, and Supercomputing Institute, University of Minnesota, Minneapolis, Minnesota 55455-0431, USA

(Received 28 April 2013; accepted 6 June 2013; published online 25 July 2013)

We present a global ground-state potential energy surface for N_4 suitable for treating high-energy vibrational-rotational energy transfer and collision-induced dissociation in N_2–N_2 collisions. To obtain the surface, complete active space second-order perturbation theory calculations were performed for the ground singlet state with an active space of 12 electrons in 12 orbitals and the maug-cc-pVTZ triple zeta basis set. About 17 000 *ab initio* data points have been calculated for the N_4 system, distributed along nine series of $N_2 + N_2$ geometries and three series of $N_3 + N$ geometries. The six-dimensional ground-state potential energy surface is fitted using least-squares fits to the many-body component of the electronic energies based on permutationally invariant polynomials in bond order variables. © *2013 AIP Publishing LLC*. [http://dx.doi.org/10.1063/1.4811653]

I. INTRODUCTION

Energy transfer and dissociation in collisions of nitrogen molecules are important for many atmospheric processes. The present motivation for studying such collisions is the role they play within the shocked gases surrounding hypersonic vehicles in establishing non-Boltzmann internal energy distributions that must be understood to model convective heat flow to the vehicle.[1] The shocked gases surrounding hypersonic vehicles are very hot and can have temperature up to 20 000 K. The high-energy collisions of the hot N_2 (molecules with high vibrational–rotational quantum numbers v, j) can involve vibrational-rotational excitation and relaxation,

$$N_2(v_1, j_1) + N_2(v_2, j_2) \rightarrow N_2(v'_1, j'_1) + N_2(v'_2, j'_2)$$

and collision-induced dissociation,

$$N_2(v_1, j_1) + N_2(v_2, j_2) \rightarrow N_2(v'_1, j'_1) + N + N.$$

The first step in molecular dynamics studies of such collisions is to obtain a potential energy surface (PES) valid up to high energy and large vibrational extensions. Ultimately one must consider coupled potential energy surfaces and electronic as well as vibrational–rotational inelasticity. However, the goal of the research reported here is to obtain a reasonably accurate global PES for the ground electronic state.

A potential energy surface for N_4 includes an N_3 surface as a subset. There have been a number of studies for the structures and energetics of N_3 species.[2–4] The dissociation of N_3 has been studied previously[5–7] and several PESs of N_3 have been reported in literature. A London-Eyring-Polanyi-Sato (LEPS) PES for the quartet state of N_3 was developed by Laganà *et al.*[8] for the classical trajectory study of N (^4S) + N_2 ($^1\Sigma_g^+$) collisions. The LEPS PES yields a collinear transition structure, which does not agree with the bent transition structure suggested by theoretical studies with multireference configuration interaction.[2] In order to improve the LEPS PES for the transition structure, the same group developed a series of new PESs[9,10] (denoted as L0 to L4), with the latest L4 PES[10] being fitted to 56 CCSD(T)/aug-cc-pVTZ energies. In 2003, Wang *et al.*[11] proposed the first full-dimensional *ab initio* based PES for N_3 $^4A''$ state for the quantum dynamics study of N (^4S) + N_2 ($^1\Sigma_g^+$) collisions. An analytic PES with 68 parameters was fitted by using 3326 points calculated by open-shell CCSD(T) with cc-pVQZ basis set. A very accurate global PES for the ground $^4A''$ state of N_3 was reported in 2007 by Galvão and Varandas[12] based on the double many-body expansion; 1592 points were calculated with CCSD(T) and MRCI+Q and extrapolated to complete basis set (CBS) limit.

Since the ground state of N_3 radical is a doublet,[7] the PESs of doublet N_3 have also attracted much attention. In 2004, an adiabatic PES for the lowest $^2A''$ state of N_3 was constructed by Babikov *et al.*[13] using tensor product B-cubic spline representation based on 2286 points calculated by MRCI+Q with aug-cc-pVTZ basis set. Adiabatic PESs for five low-lying doublet states (three $^2A'$ states and two $^2A''$ states) of N_3 have been fitted by Zhang *et al.*[14] based on 1504 points calculated by MRCI+Q with the aug-cc-pVTZ basis sets. The most recent adiabatic PESs for the two lowest $^2A''$ states of N_3 have also been developed by Galvão and Varandas[15] in 2011 with the double many-body expansion fitting strategy and used for a quasi-classical trajectory study of the N (^2D) + N_2 ($^1\Sigma_g^+$) reaction.

Several studies have been reported for the tetrahedral form of N_4,[16–18] which is considered to be a high energy density material. Theoretical geometries, energies, and physical properties have been reported.

Ab initio studies of van der Waals N_2–N_2 have also been reported. Couronne and Yellinger[19] have reported a study of the structure and stability of the $(N_2)_2$ complex at canted (taken from the crystal structure), T-shaped, X-shaped, parallel, and linear structures. The geometry of each dimer conformation was defined by four parameters, the distance between the centers of mass, two angles, and one dihedral angle,

a)Email: truhlar@umn.edu

and symmetry-constrained optimization of each conformer was carried out, where only the distance between centers of mass was optimized. T-shaped and canted conformers were found to be the most stable ones. The equilibrium structure, potential energy surface, and van der Waals mode vibration of several $(N_2)_2$ configurations have been studied with coupled cluster with singles, doubles, and quasiperturbative triples (CCSD(T)) method and quadruple zeta basis set cc-pVQZ by Wada *et al.*[20]

Unlike N_3, for which there has been considerable work on the full-dimensional *ab initio* PESs for both doublet and quartet states, very few studies have been carried out for the full-dimensional PESs of N_4. There are, however, many studies on the reduced four-dimensional PESs of N_4 for N_2–N_2 intermolecular interactions with rigid N_2 molecules in literature.[21–31] One of the first *ab initio* PES of N_2–N_2 was developed by Böhm and Ahlrichs.[21] They fitted a 4D PES with a site–site ansatz (three sites per molecule) for rigid N_2 to 46 dimer interaction energies that were calculated by the coupled-pair functional (CPF) modification of the CISD method with a [6s4p2d] basis set. Van der Avoird *et al.*[22] proposed a 4D PES in terms of spherical harmonic expansions to fit 225 *ab initio* data points. Two empirical parameters were introduced to reproduce the experimental second virial coefficients. By changing five parameters to fit several experimental properties, such as second virial coefficients, scattering crossing sections, etc., the PES was further improved by Cappelletti *et al.*[24]

Stallcop and Partridge[23] calculated N_2–N_2 interaction energies using CCSD(T) calculations with an extensive basis set, with a size of at least [6s5p4d]. An analytical PES was constructed with spherical harmonic expansions to fit the *ab initio* data. Some parameters of the PES were adjusted to experimental data to yield reliable second virial coefficients. Leonhard and Deiters[25] performed CCSD(T) calculations with aug-cc-pV*n*Z (n = D and T) basis sets and extrapolated the results to the CBS limit. They applied a site-site potential function with five sites per molecule to fit the CCSD(T)/CBS energies; two scaling parameters were introduced to reproduce the experimental second-order virial coefficients.

Aquilanti *et al.*[26] reported an experimental PES and calculated rovibrational levels of the N_2–N_2 dimer, obtained from multiproperty analysis of scattering data and second virial coefficients. In 2008, Cappelletti *et al.*[30] developed a PES using a bond-bond pairwise additive representation by combining symmetry adapted perturbation theory (SAPT) results and experimental properties. Karimi-Jafari *et al.*[27] performed MP2 calculations with basis sets up to cc-pVQZ and extrapolated the MP2 results to the CBS limit. An analytical PES based on spherical harmonic expansions was then fitted to the MP2/CBS results.

Strąk and Krukowski[28] calculated 315 geometries using CCSD(T) with the aug-cc-pVQZ basis set. The CCSD(T) results were used to parameterize an analytic PES with spherical harmonics expansions. Gomez *et al.*[29] applied the SAPT method with a [5s3p2d1f] basis set to calculate the interaction energies of nearly 460 points on the N_2–N_2 ground state. An analytical PES with spherical harmonic expansions was parameterized to those *ab initio* data.

The most recent and accurate PES of N_2–N_2 was developed by Hellman in 2012.[31] Hellman performed CCSD(T) calculations with basis sets up to aug-cc-pV5Z supplemented with bond functions; the results were further extrapolated to the CBS limit. Corrections for core-core and core-valence correlations, relativistic effects, and higher-order excitations up to CCSDT(Q) were also considered. A 4D PES was parameterized from 408 high-level *ab initio* points. Several N_2–N_2 PESs were tested for the R-dependence of anisotropy against CCSD(T) with aug-cc-pVTZ and bond functions.[32] It was shown that the potentials with simplified functional forms and parameters based on or extracted from experimental data do not reproduce the correct anisotropy of the PES and *ab initio* based PESs should be the proper way to go.

All the PESs discussed above are reduced 4D PESs with rigid N_2 molecules. We cannot use them to study high-energy collisions of N_2 with N_2 where vibrational energy transfer or collision-induced dissociations are involved. The very old PES extracted from experimental data by Johnson *et al.*[33] is one of the very few PESs of N_4 that allows one to study high-energy N_2–N_2 collisions. Morse potentials were used to model the N_2 bond stretches while exponential-six atom–atom potentials were used to model the nonbonding interactions. To the best of our knowledge, no *ab initio*-based full-dimensional PES has been reported for N_4. A distinguishing feature of the present study is the attempt to develop a full-dimensional PES valid up to high energy and large vibrational extensions of each N_2 subsystem.

Most of the PESs mentioned above were constructed with spherical harmonics, which can describe the isotropic and anisotropic intermolecular interactions of N_2 very well. Spherical harmonic expansions are a natural choice to represent reduced PESs describing the intermolecular interactions when the N_2 molecules are well separated and each close to its equilibrium internuclear distance. But this is not the case for global PESs where the dissociation of N_2 molecules is allowed. The Sorbie-Murrell[34] and Aguado-Paniagua[35] functional forms are widely used in the PES fitting of triatomic systems. Both of them involve many-body expansions that can treat the short-range and long-range interactions properly and can be constructed to have the proper asymptotic behaviors. Sorbie-Murrell and Aguado-Paniagua many-body expansions have also been used to construct the PES of tetra-atomic or penta-atomic systems, such as H_4,[36,37] H_5,[38] H_5^+,[39] but their applications are limited to monovalent atoms. For an adequate treatment of systems with complex spin-couplings of asymptotic fragments, as in current case of N_4, which could involve quartet N_3 + quartet N or doublet N_3 + doublet N, some geometry-dependent switching functions,[34] that could be very system-dependent, would have to be used.

Our approach is to use *ab initio* electronic structure theory to calculate the PES at selected geometries and then to fit this data to a global analytic function. Because we want the PES to be valid even for dissociative collisions and even near state crossings, we use a multireference wave function method that treats both static and dynamic correlation, in particular complete active space second-order perturbation theory[40,41]

(CASPT2). The fitting is accomplished using permutation-symmetry-invariant polynomials involving powers of functions of the internuclear distances. This method was pioneered by Brahms and Bowman,[42,43] who developed methods for generating the polynomials by monomial symmetrization.

This paper is organized as follows. Section II.A presents the methods used for the electronic structure calculations; Sec. II.B presents the methods used for fitting; Sec. III presents the results; Sec. IV presents the discussion; and Sec. V presents the summary.

II. METHODS

II.A. Electronic structure calculations

Multireference second order perturbation theory, in particular, CASPT2,[40,41] is used for the calculations in order to account for dynamical correlation. For the N_2 molecule, the ground state is $^1\Sigma_g^+$, and the excited electronic states are well separated in energy.[44,45] Therefore, single-state CASPT2 calculations are performed with the complete active space self-consistent field (CASSCF)[46] reference wave function optimized for the ground state.

In order to select a reasonable active space for the reference CASSCF wave function and to check the dissociation energies obtained with CASPT2, we performed test calculations for N_2 dissociation placing only 2p orbitals in the active space (active space of six electrons in six orbitals: 6e/6o) and placing both 2s and 2p orbitals in the active space (10e/8o). In the former case, the 2s orbitals were not correlated in either the SCF step or the PT2 step. The (6e/6o) CASPT2 calculation with only 2p orbitals active and correlated yielded a dissociation energy of 228.7 kcal/mol, whereas the CASPT2 dissociation energy with both 2s and 2p orbitals active and correlated is 220.3 kcal/mol. Both calculations lead to reasonably good agreement with experimental data for the dissociation energy and equilibrium bond length of nitrogen molecule (228.4 kcal/mol and 1.098 A, respectively).[44,47] However, placing 2s orbitals in the active space results in high computational costs because it leads to too many configurations. Fortunately, excluding the 1s and 2s orbitals from both the active space and PT2 correlation calculation gives an almost perfect dissociation energy for N_2. Therefore, we chose a 12e/12o active space for the N_4 system and did not correlate either 1s or 2s electrons. For nonsymmetric geometries, this leads to 40 609 128 contracted configurations. Although the eight lowest-energy orbitals (1s and 2s) are doubly occupied in all configurations, they are fully optimized for each geometry. All electronic structure calculations are performed with the MOLPRO software package.[48,49]

The calculations are carried out at sequences of geometries in which one internal coordinate is scanned while the rest of the coordinates are fixed. The Hartree–Fock wave function is used as an initial guess for the CASSCF reference wave function at the first point of each scan; then, for each of the rest of the points of the scan, the CASSCF reference wave function of the previous point is used as the starting point for the next CASSCF calculation.

For some geometrical arrangements an excited state approaches closely to the ground state. Therefore, a level shift[50] of 0.3 hartree is applied in all CASPT2 calculations in order to eliminate intruder-state problems. The g4 version of the Fock-operator,[49] which is an extension of the g1, g2, and g3 zeroth-order Hamiltonians proposed by Andersson,[51] is selected. This modified Fock-operator makes CASPT2 calculations approximately size extensive in the case of the dissociation of a molecule to high-spin open-shell atoms, which is precisely what is needed here.

The minimally augmented correlation-consistent polarized valence triple zeta basis set, maug-cc-pVTZ,[52] is used for all calculations.

For some geometries, the 2p orbital from the active space switches place with one of the 2s inactive orbitals (not included in the active space), leading to an inconsistent solution to the CASSCF equations. For N_4 this problem mostly occurs at points with high symmetry and when four nitrogen atoms are close to each other, especially in the case of (N_3 + N)-like geometries. Distorting the geometry by a small amount or using a better initial guess of the wave function helps to avoid this problem.

Occupation restrictions (restriction cards[49]) for the inactive orbitals are used in CASSCF calculations to restrict the occupation patterns in order to avoid so-called primary space (P-space) problems and CASSCF convergence problems. These problems can occur because of the limited active space or if two electronic states in the same symmetry are almost degenerate, for example near avoided crossings. However, in our case increasing the active space would make the cost prohibitive, and increasing the primary space threshold or changing configurations did not help to avoid the problem. However, restrictions solved the problem. For example, we restrict 2s inactive orbitals to have a maximum and minimum number of electrons equal to 2. Because restricted orbitals are not in the active space, this restriction does not change the result, but the restriction card changes the algorithm used by the software and eliminates the problem.

The energy of two N_2 molecules infinitely separated and each at its own equilibrium distance, is taken as the zero of energy for the PES. Relative energies with respect to the zero of energy were used for the fitting.

The initial data set consists of energies for a diverse set of geometries. Nine sets of geometries correspond to an N_2 approaching another N_2, and 3 sets of geometries correspond to a triatomic molecule interacting with an atom (N_3 + N) are used.

Figure 1 shows the coordinates used to define the geometries for the N_2 + N_2 sets. In each N_2 + N_2 set, one of the N_2 molecules has a fixed bond length r_A set successively equal to the equilibrium distance of 1.098 Å, to the equilibrium distance decreased by 0.2 Å, and to equilibrium distance increased by 0.2 Å; the other N_2 is dissociating with the bond length r_B varied from 0.8 to 6.0 Å; and the distance d between the centers of mass is varied from 1 to 10 Å to account for long range interaction at large distances. Thus each set corresponds to a set of points on a three-dimensional grid. The sets differ in the internal angles, e.g., collinear, T-shaped, etc. For example, the T-shaped model has two N_2 molecules

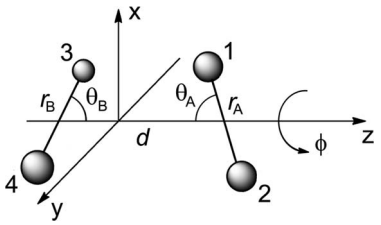

FIG. 1. Coordinates for $N_2 + N_2$. r_A: $r_e - 0.2$ Å, r_e, $r_e + 0.2$ Å, r_B: 1.0 – 5.0 Å, d: 1.0 – 10.0 Å, θ_A, θ_B: 0, $\pi/3$, $\pi/2$, φ: 0, $\pi/2$, $\pi/3$.

perpendicular to each other and situated at a distance d between their centers of mass.

In the linear $N_2 + N_2$ set and in the $N_3 + N$ sets, a different coordinate system was used; see Figure 2 where polar coordinates are used to define one of the $N_3 + N$ sets. For the triatomic molecule interacting with an atom, $^2B_1$ and $^4B_1$ bent N_3 structures were optimized with the CASPT2 (9e/9o)/maug-cc-pVTZ method. Then for each set of $N_3 + N$ calculations, the bond lengths of N_3 were fixed to the optimized values, decreased by 0.2 Å and increased by 0.2 Å. The ground-state linear $^2\Pi_g$ N_3 geometry was taken from experimental results,[53] the N–N bond lengths were set to 1.181 Å, then decreased and increased by 0.2 Å.

The sets just described lead to 16746 points. We then eliminated all points with energies greater than 2000 kcal/mol, leaving 16380 points (15363 points from $N_2 + N_2$ scanning and 1017 points from $N_3 + N$ scanning). Next we added a point corresponding to a geometry-optimized tetrahedral structure and points corresponding to optimizing cyclic and bent $^2B_1$ and $^4B_1$ structures with one N far from N_3. We also added five randomly generated points and one linear $N_3 + N$ point. And two points with short N–N bond lengths (0.6 and 0.7 Å) and a large distance between centers of mass of nitrogen molecules have been added to the data set to yield a better description of the short-bond-length repulsive region.

Finally, we added 30 points along linear synchronous transit[54] (LST) paths connecting points from two different of the 12 arrangements shown in Figure 3. For each LST path, the points on the path are generated by

$$q_i = q_i^{(0)} + \lambda\left(q_i^{(1)} - q_i^{(0)}\right),$$

where q_i is an internal coordinate, $q_i^{(0)}$ is a point from one of the systematic sets, $q_i^{(1)}$ is a point from another set, and the LST points are generated by setting the parameter λ to, for example, –0.2, +0.2, +0.4, etc. Path 1 is from an H-shaped N_4 to an X-shaped N_4; path 2 is from linear $N_3 + N$ to linear $N_2 + N_2$; path 3 is from T-shaped N_4 to X-shaped N_4 with one N_2 dissociated; and path 4 is from bent $N + N_3$ to H-shaped N_4.

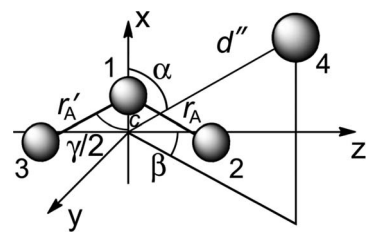

FIG. 2. Polar coordinates for the bent $^4N_3 + {}^4N$ interaction.

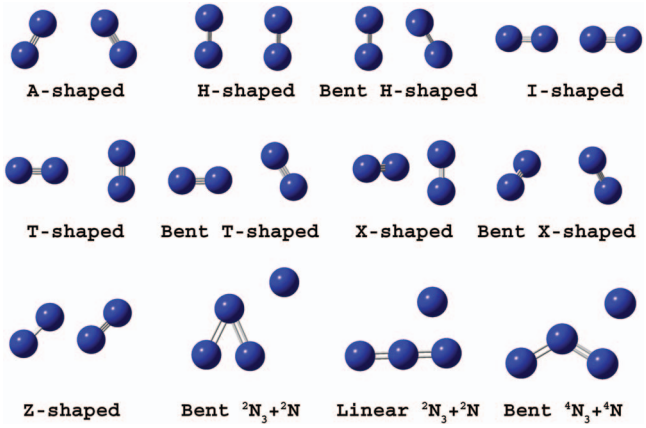

FIG. 3. Molecular arrangements for N_4.

Putting all these points together yields a total of 16421 points to be used for fitting.[55]

II.B. Fitting the potential energy surface

We defined six internuclear distances as follows: $r_1 = r_{12}$, $r_2 = r_{13}$, $r_3 = r_{14}$, $r_4 = r_{23}$, $r_5 = r_{24}$, and $r_6 = r_{34}$, where r_{ij} is the distance between atoms i and j. The variables

$$X_i = \exp(-(r_i - r_e)/a_i)$$

were used to describe the N_4 potential energy surface, where r_e is the equilibrium bond length of 1.098 Å for N_2, and r_i and a_i ($i = 1,\ldots, 6$) are internuclear distances and nonlinear parameters, respectively. Since X_i may be interpreted as a Pauling bond order,[56–60] the X_i are called bond orders. Since a quadratic polynomial in X_i is equivalent to a Morse curve,[61] they may also be called Morse variables.

We chose 0.9 Å for all a_i based on some trial tests. The starting point for an analytic PES is an expansion in a Taylor series of bond orders as

$$V(r_1, r_2, r_3, r_4, r_5, r_6) = \sum_{n_1+n_2+n_3+n_4+n_5+n_6=0}^{k} C_{n_1n_2n_3n_4n_5n_6} \times X_1^{n_1} X_2^{n_2} X_3^{n_3} X_4^{n_4} X_5^{n_5} X_6^{n_6}, \quad (1)$$

where n_i is the order of polynomial of X_i, and the coefficients $C_{n_1n_2n_3n_4n_5n_6}$ are the linear parameters that need to be determined through least-squares fits. The summation in Eq. (1) is over all n_1, n_2, n_3, n_4, n_5, and n_6, each starting from 0, such that their sum is less than or equal to k; therefore, k is the highest total degree of the multinomials. Due to the permutation symmetry of the four identical N atoms, some of the coefficients are identical by symmetry. One can therefore construct an explicitly permutationally invariant basis to reduce the number of linear coefficients.[42,43] In the present paper, we follow the monomial symmetrization approach proposed

by Xie and Bowman[62] to construct permutationally invariant polynomial basis functions to fit the global potential energy surface of N_4. Furthermore we required the fit to reduce to the energy V_0 of four atoms at complete dissociation, we removed terms in Eq. (1) that are products of unconnected distances, and we replaced terms that only describe pairwise 2-body interactions by a pre-optimized N_2 potential energy function. This yields

$$V(r_1, r_2, r_3, r_4, r_5, r_6) = V_0 + \sum_{i=1}^{6} V_2(r_i) + \sum_{\substack{k \\ \text{connected} \\ n_1+n_2+n_3+n_4+n_5+n_6=2}} D_{n_1 n_2 n_3 n_4 n_5 n_6} S\left[X_1^{n_1} X_2^{n_2} X_3^{n_3} X_4^{n_4} X_5^{n_5} X_6^{n_6}\right], \quad (2)$$

where $S[X_1^{n_1} X_2^{n_2} X_3^{n_3} X_4^{n_4} X_5^{n_5} X_6^{n_6}]$ are the symmetrized permutation-invariant polynomial basis functions, and $D_{n_1 n_2 n_3 n_4 n_5 n_6}$ are the linear coefficients. Further details are in supplementary material.[55]

We truncated the Taylor expansion at $k = 9$. This includes 5005 terms if one uses Eq. (1); however, by removing 2-body and unconnected terms and using symmetrized polynomials $S[X_1^{n_1} X_2^{n_2} X_3^{n_3} X_4^{n_4} X_5^{n_5} X_6^{n_6}]$ as the $k = 9$ basis, the number of independent terms is reduced to 276. The 276 coefficients $D_{n_1 n_2 n_3 n_4 n_5 n_6}$ are determined by least-square fits.

Since we are interested in high-energy collisions, we need to fit our potential energy surface over a very wide energy range. To avoid putting too much emphasis on the high-energy data points and reducing the fitting quality of data points with relatively low energies, we reduced the weight on high-energy points, as has been done before.[63] However, in the present work we used a newly devised weighting function; in particular, we use the following weighting factor in our weighted-least-square fitting:

$$w(i) = \begin{cases} 1 & \text{for } E_i \le E_c \\ E_c^2/E_i^2 & \text{for } E_i > E_c \end{cases}, \quad (3)$$

where $w(i)$ is the weighting factor of data point i with energy E_i, and E_c is a preselected energy threshold to reduce the weights of high-energy data points. In the final fit, we chose E_c to be 100 kcal/mol. Furthermore, we excluded the data points with energies larger than 2000 kcal/mol in our fitting. We think that energies above 2000 kcal/mol would be rarely visited during dynamic studies, and the accuracy in those ranges is not very important.

III. RESULTS

Figures 4(a)–4(d) show comparisons of the global fit to the calculated points on the dissociation curves for N–N interacting with N_2, where the calculations are performed with the CASPT2 method for various dimer arrangements. Results are given as a function of the internuclear distance in one molecule (r_B) with the other molecule (r_A) at its equilibrium distance. Although we do not show plots to illustrate this, the fits also include data like this with the second molecule stretched by 0.2 Å from its equilibrium geometry and with it compressed by 0.2 Å from its equilibrium geometry. Seven more plots similar to Figures 4(a)–4(d) for other geometries are given in the supplementary material.[55] A surface cut as a function of two variables is shown in Figure 5 for the bent T-shaped dimer. The surface cut is not from the global fit, but rather is based on local interpolation to guide the eye in visualizing the data.

The root-mean-square errors (RMSEs) and mean unsigned errors (MUEs) of the final fit are shown for different energy ranges in Table I.

The results in Table I are for the final fit to all the data. To further test the quality of our fitted PES, we omitted the data corresponding to the four LST paths to see how our fitting procedure would perform for data quite different from that used in the fit. The energies predicted by this test fit, as well as the CASPT2 energies being predicted, are shown in Figure 6.

IV. DISCUSSION

As a subset of the N_4 surface, the surface of N_3 interacting with an atom has been calculated. Therefore, stationary points of N_3 were used. The geometries of low-lying cyclic $^2B_1$ and bent $^4B_1$ stationary structures were taken from a recent work[7] and optimized with CASPT2. Our optimized nonlinear stationary structures of N_3 agree well with previous theoretical results. For $^2B_1$ calculated bond lengths are 1.45 Å and N–N–N angle is 50.2°. For $^4B_1$, the bond lengths are 1.27 Å and N–N–N angle is 117.4°.

For comparison with previous studies of tetrahedral N_4, we performed an optimization of the tetrahedral structure of singlet N_4 at the CASPT2(12e/12o)/maug-cc-pVTZ level. The bond lengths and absolute energy obtained with the method we used are consistent with previous computational work:[18] the N–N bond length is 1.450 Å, the energy, relative to two nitrogen molecules, is 191.7 kcal/mol. At this geometry the fit gives an energy of 173.4 kcal/mol, with an error of 18.3 kcal/mol. Although not very good, the fit is still acceptable. Actually, the large discrepancy of relative energies of the tetrahedral N_4 calculated by CASPT2 and our analytic PES is an example of a more general phenomenon, namely that the fit is less accurate near surface crossings where the fitted PES smooths out the cusp due to state crossing, as shown clearly in

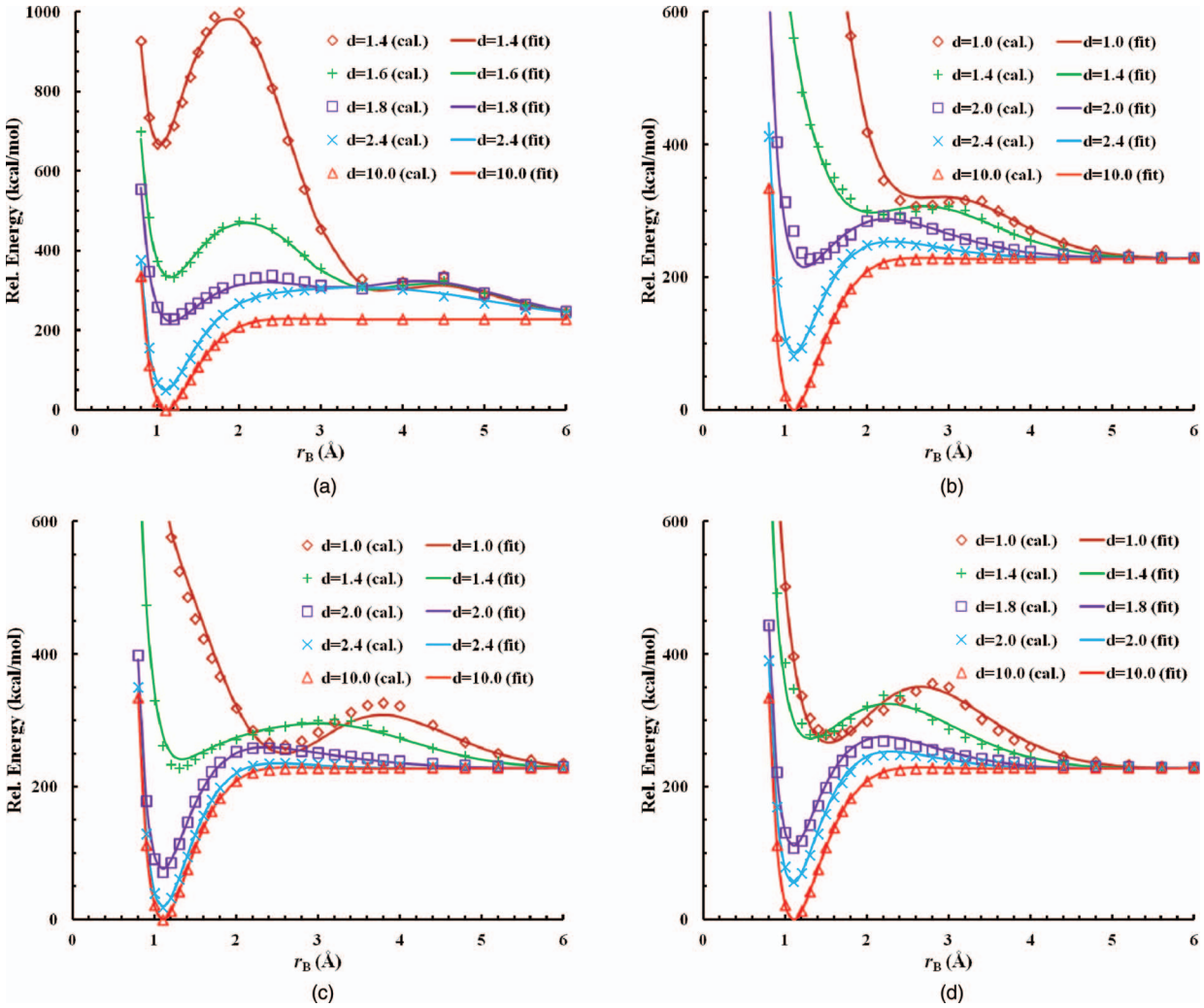

FIG. 4. (a) Dissociation curves for $N_2 + N_2$: comparison of the global fit to the values obtained with the CASPT2 method for the A-shaped set with one N_2 fixed to its equilibrium distance. Both r_B and d are in Å. In all figures, d is the distance between the centers of mass of the two nitrogen molecules. (b) Dissociation curves for $N_2 + N_2$: comparison of the global fit to the values obtained with the CASPT2 method for the T-shaped set with one N_2 fixed to its equilibrium distance. (c) Dissociation curves for $N_2 + N_2$: comparison of the global fit to the values obtained with the CASPT2 method for the H-shaped set with one N_2 fixed to its equilibrium distance. (d) Dissociation curves for $N_2 + N_2$: comparison of the global fit to the values obtained with the CASPT2 method for the X-shaped set with one N_2 fixed to its equilibrium distance.

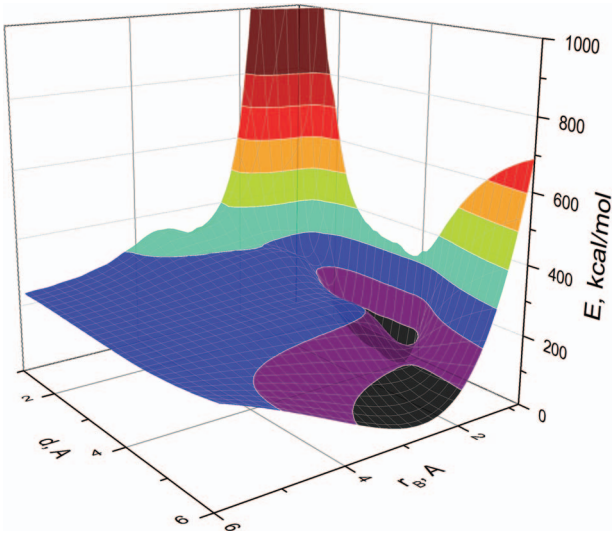

FIG. 5. Three-dimensional surface for $N_2 + N_2$, obtained with the CASPT2 method for bent T-shaped arrangement.

Figure 4(d) for $d = 1.0$ and 1.4 Å, respectively, where d is the distance between the centers of mass of the two N_2 molecules. Our goal here is to fit the lowest adiabatic potential energy surface, even though that surface has cuspidal ridges due to surface crossings, and the functional form chosen here, with continuous derivatives, must smooth those crossings out. This could be considered a disadvantage or an advantage, with the

TABLE I. The mean unsigned errors (MUEs) and root-mean-square errors (RMSEs) of the fitted potential energy surface with respect to CASPT2/maug-cc-pVTZ results for different energy ranges (in kcal/mol).

	Number of points	MUE	RMSE
$E < 100.0$	693	1.3	1.8
$100.0 \le E < 228.0$	1939	2.3	4.1
$228.0 \le E < 456.0$	11 849	3.6	7.2
$456.0 \le E < 1000.0$	1607	12.8	18.0
$E > 1000.0$	333	40.4	81.2
All data	16 421	5.0	14.3

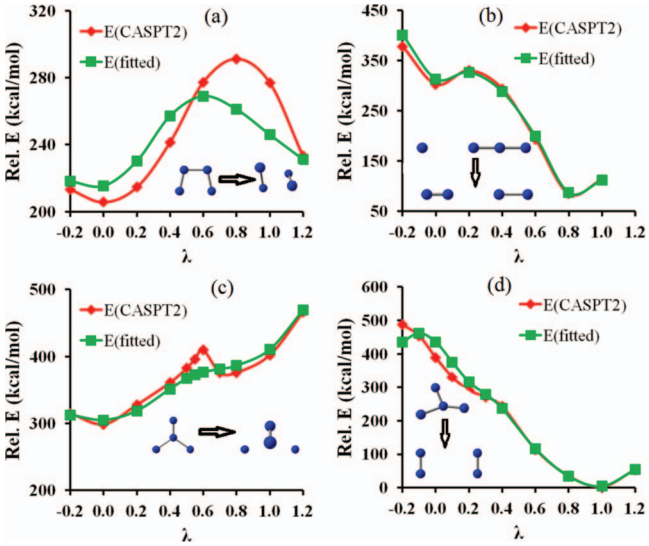

FIG. 6. Comparison of the test fit (green) to the CASPT2/maug-cc-pVTZ data (red) for the four LST paths. (The data points along the 4 paths are not included in the test fit to see the ability of the fitting strategy to predict the relative energies of N_4.)

latter point of view reflecting the fact that Born-Oppenheimer trajectories will be smoother (and hence probably more realistic) if one smooths the cuspidal ridges. The only truly satisfactory way to fit potential energy surfaces in the presence of surface crossings is to use a diabatic representation and fit more than one surface and their couplings,[64,65] but that is beyond the scope of the present study.

Table I shows that the average quality of the fitted PES is quite good since the RMSE for $E < 100$ kcal/mol is only 1.8 kcal/mol, and the RMSE for 100 kcal/mol $\leq E < 228$ kcal/mol is 4.1 kcal/mol. The RMSE is a good criterion for evaluating the fitting accuracy if the errors are normally distributed. However, it could be exaggerated by larger errors, and the MUEs are more robust. That is why Table I also provides the MUEs for the various energy ranges. The MUEs are quite small, 1.3 kcal/mol for $E < 100$ kcal/mol and 2.3 kcal/mol for 100 kcal/mol $\leq E < 228$ kcal/mol. Both RMSEs and MUEs show that our fitted PES is quite good (better than the expected accuracy of CASPT2) for energies below the dissociation limit of 228 kcal/mol. For 228 kcal/mol $\leq E < 456$ kcal/mol, our fitting is still quite good, with RMSE and MUE of 7.2 and 3.6 kcal/mol, respectively. So our PES should be suitable to study high-energy collisions of N_2 with N_2.

The quality of the fitting procedure was further tested by leaving the 30 LST points out of the fitting process, producing a less accurate global surface called the test PES. The test surface reproduces the general trends of the CASPT2 curves for the LST paths. The agreement of energies predicted by the test PES and those calculated by CASPT2 is best for energies lower than the dissociation limit (228 kcal/mol), as also implied by the RMSEs and MUEs of the final fit. Path 1 calculated by CASPT2 has an energy maximum at $\lambda = 0.8$. The energy maximum has been shifted to $\lambda = 0.6$ with the test PES. But the qualitative shape of path 1 predicted by our test PES agrees with that calculated by CASPT2. Path 2 predicted by our test PES agrees extremely well with the CASPT2 one, especially for the data points with energies below 300 kcal/mol. The test PES reproduces path 3 near the starting T-shaped N_4, but it fails to reproduce the cusp due to a state crossing near $\lambda = 0.6$. Instead, it yields a smooth curve near the cusp. That problem, discussed above for the final fit, is inevitable when one fits adiabatic surfaces to continuous functions, as has been observed before.[66] For path 4, the test fit reproduces the CASPT2 curves very well for energy below 300 kcal/mol, but the agreement degrades for higher energies.

V. SUMMARY

A global ground-state potential energy surface for N_4 suitable for treating high-energy vibrational-rotational energy transfer and dissociation in N_2–N_2 collisions has been calculated by the CASPT2 method and fitted using least-squares fits to electronic energies based on permutationally invariant polynomials in bond orders. The data used for the fit include nine sets of ($N_2 + N_2$)-type geometries and three sets of ($N_3 + N$)-type geometries, plus four paths connecting points in different sets and selected optimized and random geometries. A Fortran subroutine of the N_4 PES is available in the POTLIB library.[67,68]

ACKNOWLEDGMENTS

The authors are grateful to Boris Averkiev, Jason Bender, Graham V. Candler, Sriram Doraiswamy, and Antonio Varandas for symbiotic collaboration on overlapping projects, to Bas Braams for helpful correspondence, and to Zhen Xie and Joel M. Bowman for the help with their effective monomial symmetrization approach (EMSA) program to generate the explicitly symmetrized permutationally invariant polynomial basis functions. This work was sponsored by the Air Force Office of Scientific Research (AFOSR) under MURI Grant No. FA9550-10-1-0563. The views and conclusions contained herein are those of the authors and should not be interpreted as necessarily representing the official policies or endorsements, either expressed or implied, of the AFOSR or the U.S. Government.

[1] I. Nompelis, G. V. Candler, and M. S. Holden, AIAA J. **41**, 2162 (2003).
[2] C. Petrongolo, J. Mol. Struct. **175**, 215 (1988).
[3] J. N. Murrell, O. Novaro, and S. Castillo, Chem. Phys. Lett. **90**, 421 (1982).
[4] I. S. K. Kerkines, Z. Wang, P. Zhang, and K. Morokuma, Mol. Phys. **107**, 1017 (2009).
[5] J. M. L. Martin, J. P. François, and R. Gijbels, J. Chem. Phys. **93**, 4485 (1990).
[6] R. E. Continetti, D. R. Cyr, D. L. Osborn, D. J. Leahy, and D. M. Neumark, J. Chem. Phys. **99**, 2616 (1993).
[7] P. Zhang, K. Morokuma, and A. M. Wodtke, J. Chem. Phys. **122**, 014106 (2005).
[8] A. Laganà, E. Garcià, and L. Ciccarelli, J. Phys. Chem. **91**, 312 (1987).
[9] E. Garcià and A. Laganà, J. Phys. Chem. A **101**, 4734 (1997).
[10] E. Garcià, A. Saracibar, S. Gómez-Carrasco, and A. Laganà, Phys. Chem. Chem. Phys. **10**, 2552 (2008).
[11] D. Wang, J. R. Stallcop, W. M. Huo, C. E. Dateo, D. W. Schwenke, and H. Partridge, J. Chem. Phys. **118**, 2186 (2003).
[12] B. R. L. Galvão and A. J. C. Varandas, J. Phys. Chem. A **113**, 14424 (2009).
[13] D. Babikov, P. Zhang, and K. Morokuma, J. Chem. Phys. **121**, 6743 (2004).
[14] Z. Wang, I. S. K. Kerkines, K. Morokuma, and P. Zhang, J. Chem. Phys. **130**, 044313 (2009).

[15]B. R. L. Galvão and A. J. C. Varandas, J. Phys. Chem. A **115**, 12390 (2011).
[16]M. M. Francl and J. P. Chesick, J. Phys. Chem. **94**, 526 (1990).
[17]T. J. Lee and J. E. Rice, J. Chem. Phys. **94**, 1215 (1991).
[18]M. L. Leininger, T. J. Van Huis, and H. F. Schaefer III, J. Phys. Chem. A **101**, 4460 (1997).
[19]O. Couronne and Y. Ellinger, Chem. Phys. Lett. **306**, 71 (1999).
[20]A. Wada, H. Kanamori, and S. Iwata, J. Chem. Phys. **109**, 9434 (1998).
[21]H.-J. Böhm and R. Ahlrichs, Mol. Phys. **55**, 1159 (1985).
[22]A. van der Avoird, P. E. S. Wormer, and A. P. J. Jansen, J. Chem. Phys. **84**, 1629 (1985).
[23]J. R. Stallcop and H. Partridge, Chem. Phys. Lett. **281**, 212 (1997).
[24]D. Cappelletti, F. Vecchiocattivi, F. Pirani, E. L. Heck, and A. S. Dickinson, Mol. Phys. **93**, 485 (1998).
[25]K. Leonhard and U. K. Deiters, Mol. Phys. **100**, 2571 (2002).
[26]V. Aquilanti, M. Bartolomei, D. Cappelletti, E. Carmona-Novillo, and F. Pirani, J. Chem. Phys. **117**, 615 (2002).
[27]M. H. Karimi-Jafari, A. Maghari, and S. Shahbazian, Chem. Phys. **314**, 249 (2005).
[28]P. Strąk and S. Krukowski, J. Chem. Phys. **126**, 194501 (2007).
[29]L. Gomez, B. Bussery-Honvault, T. Cauchy, M. Bartolomei, D. Cappelletti, and F. Pirani, Chem. Phys. Lett. **445**, 99 (2007).
[30]D. Cappelletti, F. Pirani, B. Bussery-Honvault, L. Gomez, and M. Bartolomei, Phys. Chem. Chem. Phys. **10**, 4281 (2008).
[31]R. Hellmann, Mol. Phys. **111**, 387 (2012).
[32]M. H. Karimi-Jafari and M. Ashouri, Phys. Chem. Chem. Phys. **13**, 9887 (2011).
[33]J. D. Johnson, M. S. Shaw, and B. L. Holian, J. Chem. Phys. **80**, 1279 (1983).
[34]K. S. Sorbie and J. N. Murrell, Mol. Phys. **29**, 1387 (1975).
[35]A. Aguado and M. Paniagua, J. Chem. Phys. **96**, 1265 (1992).
[36]A. J. C. Varandas and J. N. Murrell, Faraday Discuss. **62**, 92 (1977).
[37]A. Aguado, C. Suárez, and M. Paniagua, J. Chem. Phys. **101**, 4004 (1994).
[38]C. Tablero, A. Aguado, and M. Paniagua, J. Chem. Phys. **110**, 7796 (1999).
[39]A. Aguado, P. Barragán, R. Prosmiti, G. Delgado-Barrio, P. Villarreal, and O. Roncero, J. Chem. Phys. **133**, 024306 (2010).
[40]K. Andersson, P.-Å. Malmqvist, and B. O. Roos, J. Chem. Phys. **96**, 1218 (1992).
[41]H.-J. Werner, Mol. Phys. **89**, 645 (1996).
[42]B. J. Braams and J. M. Bowman, Int. Rev. Phys. Chem. **28**, 577 (2009).
[43]J. M. Bowman, B. J. Braams, S. Carter, C. Chen, G. Czakó, B. Fu, X. Huang, E. Kamarchik, A. R. Sharma, B. C. Shepler, Y. Wang, and Z. Xie, J. Phys. Chem. Lett. **1**, 1866 (2010).
[44]F. R. Gilmore, J. Quant. Spectrosc. Radiat. Trans. **5**, 369 (1965).
[45]J. W. McGowan and H. H. Michels, Adv. Chem. Phys. **45**, 224 (1981).
[46]P. J. Knowles and H.-J. Werner, Chem. Phys. Lett. **115**, 259 (1985).
[47]K. P. Huber and G. Herzberg, *Molecular Spectra and Molecular Structure. IV. Constants of Diatomic Molecules* (Van Nostrand Reinhold Co., 1979), p. 412.
[48]H.-J. Werner, P. J. Knowles, G. Knizia, F. R. Manby, and M. Schütz, WIREs Comput. Mol. Sci. **2**, 242 (2012).
[49]H.-J. Werner, P. J. Knowles, G. Knizia, F. R. Manby, M. Schütz *et al.*, MOLPRO, version 2010.1, a package of *ab initio* programs, 2010, see http://www.molpro.net.
[50]B. O. Roos and K. Andersson, Chem. Phys. Lett. **245**, 215 (1995).
[51]K. Andersson, Theor. Chim Acta **91**, 31 (1995).
[52]E. Papajak, H. R. Leverentz, J. Zheng, and D. G. Truhlar, J. Chem. Theory Comput. **5**, 1197 (2009).
[53]C. R. Brazier, P. F. Bernath, J. B. Burkholder, and C. J. Howard, J. Chem. Phys. **89**, 1762 (1988).
[54]T. A. Halgren and W. N. Lipscomb, Chem. Phys. Lett. **49**, 225 (1977).
[55]See supplementary material at http://dx.doi.org/10.1063/1.4811653 for the full data of geometries and energies used for the fit.
[56]L. Pauling, *The Nature of the Chemical Bond*, 3rd ed. (Cornell University Press, Ithaca, NY, 1960), p. 98.
[57]H. S. Johnston, Adv. Chem. Phys. **3**, 131 (1961).
[58]A. Lagana, G. O. d. Aspuru, and E. Garcia, J. Chem. Phys. **108**, 3886 (1998).
[59]G. Lendvay, J. Mol. Struct.: THEOCHEM **501–502**, 389 (2000).
[60]M. Zhao, M. A. Iron, P. Staszewski, N. E. Schultz, R. Valero, and D. G. Truhlar, J. Chem. Theory Comput. **5**, 594 (2009).
[61]P. M. Morse, Phys. Rev. **34**, 57 (1929).
[62]Z. Xie and J. M. Bowman, J. Chem. Theory Comput. **6**, 26 (2010).
[63]A. W. Jasper, N. E. Schultz, and D. G. Truhlar, J. Phys. Chem. B **109**, 3915 (2005).
[64]S. Nangia and D. G. Truhlar, J. Chem. Phys. **124**, 124309 (2006).
[65]Z. H. Li, R. Valero, and D. G. Truhlar, Theor. Chem. Acc. **118**, 9 (2007).
[66]B. Fu, E. Kamarchik, and J. M. Bowman, J. Chem. Phys. **133**, 164306 (2010).
[67]R. J. Duchovic, Y. L. Volobuev, G. C. Lynch, T. C. Allison, J. C. Corchado, D. G. Truhlar, A. F. Wagner, and B. C. Garrett, Comput. Phys. Commun. **144**, 169–187 (2002); Erratum, **156**, 319–322 (2004).
[68]See http://comp.chem.umn.edu/potlib/ for the latest version of POTLIB that includes the N_4 potential energy surface.